Anodic Polarization Behaviour of Nickel-Based Alloys in Neutral and Very Acidic Solutions

Aezeden Mohamed, J. R. Cahoon, and W. F. Caley

Faculty of Engineering, University Manitoba, Winnipeg, Canada, R3T 5V6
amohamed@mun.ca

Abstract

Cyclic anodic polarization curves in 3.5 wt% NaCl at pH = 7.0 solution, HCl at pH = 0.0 and 10 wt% $FeCl_3$ solution at pH = 0.0 were obtained for three nickel based alloys, 600, 601 and C22. When tested in the 3.5 wt% saline solution all three alloys exhibited passive behaviour. The higher Cr content of alloy 601 (25 at %) over that of alloy 600 (17 at %) resulted in a higher pitting potential for alloy 601 and thus a higher resistance to pitting corrosion. However, the cyclic polarization curves for both these alloys in the saline solution exhibited a large amount of hysteresis indicating a susceptibility to crevice corrosion. The presence of 8 at% Mo in alloy C22 increased the pitting potential over alloys 600 and 601 and essentially eliminated the hysteresis in the cyclic polarization curves.

When tested in HCl at pH = 0.0, both alloys 600 and 601exibited active corrosion behaviour and a resultant high corrosion rate indicating these two alloys are not suitable for containment of concentrated HCl solutions. On the other hand, alloy C22 in HCl exhibited passive behaviour, high pitting potentials and little hysteresis in the cyclic polarization curves indicating that alloy C22 is suitable for containment of concentrated HCl even in the presence of crevices.

When tested in 10 wt% $FeCl_3$ solution at pH = 0.0, alloy 600 exhibited active corrosion behaviour with a resultant high corrosion rate whereas Alloy 601 exhibited two types of

corrosion behaviour. One type resulted in passive polarization behaviour very similar to the behaviour exhibited for corrosion of alloy 601 in the much less aggressive 3 wt% saline solution at pH =7.0. The second type of polarization behaviour for alloy 601 tended towards active corrosion with only a small passive region.

When tested in 10 wt% $FeCl_3$ solution at pH = 0.0, alloy C22 exhibited passive polarization behaviour with low corrosion rates and essentially no hysteresis in the cyclic polarization curves. It is concluded that alloy C22 is suitable for containment of neutral saline solutions, concentrated HCl at pH = 0.0 or higher, and 10 wt% $FeCl_3$ solution at pH = 0.0 or higher. For all three solutions, corrosion rates of alloy C22 are low, pitting potentials are high and the absence of hysteresis on the cyclic polarization curves indicate that alloy C22 has excellent general corrosion resistance and good resistance to both pitting and crevice corrosion in all three solutions tested. Alloys 600 and 601 could be used to contain neutral saline solutions although they could be susceptible to crevice corrosion. These two alloys but would be not be suitable for containment of HCl or $FeCl_3$ solutions at pH = 0 due to a tendency towards active corrosion behaviour in these solutions.

Keywords: Cyclic; Anodic; Polarization; Pitting corrosion; Nickel-based alloys

Introduction

Nickel-based alloys both with and without Mo additions are widely used in many applications because of their good corrosion resistance in a variety of very corrosive solutions and their high temperature oxidation resistance [1]. Many of the studies concerning the corrosion resistance of these alloys have concentrated on NaCl solutions with pH values above 2 and often at elevated temperatures up to 95 ^{o}C [1,2,3,4]. It is therefore of interest to investigate the corrosion properties of some nickel-based alloys in more acidic solutions in an attempt to determine the useful limits of such alloys.

Considerable information concerning corrosion characteristics can be readily obtained from cyclic anodic polarization studies. Parameters obtained from such studies include the corrosion or rest potential, E_R, the breakdown or pitting potential, E_B, the corrosion current density, I_{CORR}, the passive current density, I_{PASS}, and the protection or repassivation potential [5]. Therefore, a study was initiated to examine the corrosion behaviour of alloy 600, alloy 601 and alloy C22 using the cyclic anodic polarization technique. These alloys were chosen for their range of Cr content from 17 at. % to 25 at. % and the presence of Mo in C22 (Table 1). Three electrolytes were chosen for study. Firstly, 3.5 wt. % NaCl solution at pH = 7.0 was chosen for comparison with other investigations. Secondly, HCl acid at pH = 0.0 was utilized since this is a very acidic solution and contains considerable Cl$^-$ ions which are known to enhance crevice corrosion in some nickel-based alloys [6]. Thirdly, 10% FeCl$_3$ solution at pH = 0.0 was selected since this solution is extremely corrosive to some materials with corrosion rates for Al, Cu and mild steel greater than 20 cm per year [7].

Further, the three alloys studied have quite similar mechanical properties [8], although C22 is slightly stronger, and establishing the useful corrosion limits of these alloys may allow the use of a less expensive alloy for a particular application.

Experimental

Specimens 0.5" long were cut from 0.5" diameter bars, annealed for 1 hour at 1000 ^{o}C then mounted in Bakelite such that the exposed area was 1.29 cm^2. The exposed area was sanded to 600 grit paper, ultrasonically degreased in a detergent solution, rinsed with water then placed in an electrochemical cell containing 500 ml of electrolyte. The cell was a 500 ml Erlenmeyer flask containing the sample (working electrode), two 0.25" diameter graphite counter electrodes and a saturated calomel reference electrode (SCE). The pH of the electrolyte was adjusted by additions of HCl and NaOH. After allowing one hour for the potential to stabilize, cyclic anodic polarization scans were conducted using a Model 350A Princeton Applied Research Corrosion Measurement Instrument. The scans were initiated at a potential 250 mv below the corrosion potential and were conducted a scan rate of 1mv/sec. For the scans conducted in 3.5 wt. % NaCl solution at pH = 7.0, the scan was reversed when the anodic current density reached a value of 5.0 x 10^6 nA/cm^2. All other scans were reversed when the potential reached 1.2 V vs. SCE. The reverse scans were continued until the potential was reduced to that of the corrosion potential or below. All runs were repeated in triplicate.

Results and discussion

Cyclic polarization curves for alloy 600, alloy 601 and alloy C22 in 3.5 wt. % NaCl solution at pH = 7.0 are given in Figs. 1 to 3 respectively. Curves for the three alloys in HCl at pH = 0.0 are presented in Figs. 4 to 6 and for polarization in 10 wt. % FeCl$_3$ at pH = 0.0 in Figs. 7 through 9.

The various parameters obtained from cyclic anodic polarization studies of relevance to corrosion behaviour are given in Table 2. These are:

1. The rest or corrosion potential, E_R, taken as the potential at which the current changes from cathodic to anodic on the forward scan;

2. The breakdown or pitting potential, E_B, taken, for purposes of this investigation, as the potential at the intersection of the linear extrapolations of the passive region current and the trans-passive region current;

3. The corrosion current density taken, for purposes of this investigation, as the current at the intersection of the of the linear extrapolation of the cathodic Tafel slope with the rest potential;

4. The passive current density taken as the current in the passive region on the forward scan midway between the breakdown and rest potentials;

5. The protection potential taken as the potential at the first intersection of the reverse scan with the passive current density.

The corrosion rate, R, taken as the depth of corrosion penetration per year in mm is given by

$$R = \frac{(327 \, I_{CORR} \, A_W)}{(\rho \, N)} \, . \tag{1}$$

In Eq. (1), I_{CORR} is the corrosion current density (in A/cm^2), A_W is the atomic weight of the alloy, ρ is the density and N is the valence or oxidation state.

The values of A_W, ρ, and N are dependent upon the composition of the alloy. For purposes of this investigation the contribution of each of the elements in the alloy is taken as linearly proportional to its atomic fraction. The values used for each of the constituents in the alloy are included in Table 1. The numeric constant, 327 in Eq. (1), contains the number of seconds in a year, the

Faraday constant (F = 96,485 coulombs per gram equivalent weight), and the factor of 10 converting cm to mm. The values of A_W, ρ, and N for each of the alloys used in this investigation are given in Table 3.

With respect to susceptibility of a metal or alloy to pitting corrosion, it is not the value of the pitting potential per se that is important but the difference between the pitting potential, E_B, and the corrosion or rest potential, E_R. The higher the value of $E_B - E_R$ the less the susceptibility to pitting corrosion. Similarly, the susceptibility of a metal or alloy to crevice corrosion is indicated by the amount of hysteresis in the cyclic polarization curve. A measure of the amount of hysteresis is given by the difference of the protection potential, E_P, and the rest potential, E_R. A high value of $E_P - E_R$, (approaching the value of $E_B - E_R$), is an indication of resistance to crevice corrosion. A summary of the values of $E_B - E_R$ and $E_P - E_R$ is presented in Table 4.

For corrosion in 3.5 wt % saline solution at pH = 7.0, all alloys exhibited passive behaviour with low corrosion rates in the range 0.02 - 0.05 mmpy. With respect to pitting corrosion, alloy 600 with 17 at % Cr (Table 1) has the least resistance with a value for $E_B - E_R = 0.398$ V (Table 4). Increasing the Cr content in alloy 601 to 25 at% Cr over the value of 17 at% Cr in alloy 600 increases the value of $E_B - E_R$ to 0.490 V compared to the value of $E_B - E_R = 0.398$ V for alloy 600. Therefore, alloy 601 likely has increased resistance to pitting corrosion over alloy 600 in 3.5 wt% NaCl solution at pH = 7.0.

Alloy C22 with essentially the same Cr content as alloy 601 (25 at% as given in Table 1) but with the addition of 8.57 at% Mo exhibits a value of $E_B - E_R = 0.736$ V as indicated in Table 4. Therefore, the presence of Mo in alloy C22 is very effective in increasing the resistance to pitting corrosion in 3.5 wt% NaCl solution.

It should be noted that alloy C22 contains 1.33 at% W as well as 8.57 at% Mo. Tungsten has a very similar outer electron structure to that of Mo and therefore may contribute to the pitting potential of the alloy. Actually, the ground state of a single atom of W has an outer electron configuration $5d^4 6s^2$ while Mo has a $4d^5 5s^1$ configuration [9]. However, as pointed out by Engel and Brewer [10], in the solid state, the $6s^2$ configuration is a completed sub shell and not well suited for bonding, Therefore, only the $4d^4$ electrons would be available for bonding. However, in the solid state, one of the $6s^2$ electrons is promoted to the 5d shell resulting in a $5d^5$ $6s^1$ configuration with 6 bonding electrons. The increase in bonding energy due to the 6 electrons available for bonding more than offsets the promotion energy required for the 6s to 5d electron transition. Therefore, in the solid state tungsten may well behave similarly to molybdenum.

With respect to crevice corrosion in saline solution, both alloy 600 and alloy 601 exhibit a large hysteresis in their cyclic polarization curves as shown in Figs. 1 and 2, and low values for the protection potential, E_p, resulting in low values for $E_P - E_R \approx 0.150$ V (Table 4) indicating a susceptibility towards crevice corrosion. Alloy 22 however, however, shows almost no hysteresis (Fig. 3) and a resultant high value for $E_P - E_R = 0.765$ V which is essentially equivalent to the value of $E_B - E_R = 0.736$ V (Table 4). Therefore, alloy 22 is expected to be have good resistance to both pitting and crevice corrosion in 3.5 wt% saline solution at pH = 7.0.

The cyclic polarization behaviour for the three alloys tested in HCl at pH = 0 presented in Figs. 3 to 5 shows that alloys 600 and 601 exhibit active corrosion behaviour with much higher corrosion rates than for the alloys tested in 3.5 wt% NaCl solution. However, the corrosion rates for these two alloys in HCl at pH = 0.0 calculated via cathodic Tafel extrapolation is probably considerably lower than would actually occur in service under these conditions. Figs. 4 and 5 show that the breakdown or pitting potentials for both alloys 600 and 601 in HCl at pH = 0.0 is

essentially the corrosion potential and therefore considerable pitting corrosion would likely occur

raising the actual corrosion rate.

The cyclic polarization curve for alloy C22 in HCl at pH = 0.0 presented in Fig. 6 shows

that alloy C22 exhibits passive behaviour in this environment. Further, corrosion rates are low

(Table 2) and the parameters $E_B - E_R$ and $E_P - E_R$ (Table 4) are very similar to the values

obtained for this alloy in the much less aggressive 3.5 wt% NaCl solution. Also, the cyclic

polarization curve (Fig. 6) shows little hysteresis indicating a good resistance to crevice

corrosion. The excellent corrosion resistance of alloy C22 in HCl at pH = 0.0 compared to that of

alloy 601 is clearly due the presence of Mo in alloy C22.

The cyclic polarization curve for alloy 600 in 10 wt% $FeCl_3$ at pH = 0.0 solution is given

in Fig. 7 which shows that alloy 600 undergoes active corrosion in this solution. The corrosion

rate determined from cathodic Tafel extrapolation is high, 3.30 mm/year, (Table 2) and, as for

alloy 600 in HCl at pH = 0.0, the rest potential is essentially the pitting potential. Therefore,

considerable pitting corrosion of alloy 600 would likely occur in this environment increasing the

actual corrosion rate.

Alloy 601 exhibited two types of polarization behaviour when tested in 10 wt% $FeCl_3$ at

pH = 0.0. Type "a" behaviour given in Fig. 8a shows passive behaviour with corrosion

parameters very similar to those for alloy 601 tested in 3.5 wt% NaCl solution at pH = 7.0 with

values of $E_B - E_R = 0.560$ V and $E_P - E_R = 0.010$ V The large hysteresis of the cyclic

polarization curve indicates that alloy 601 would be also be susceptible to crevice corrosion in

this solution.

The second type of polarization behaviour (type "b") for alloy 601 in 10 wt% $FeCl_3$

solution at pH = 0.0 is shown in Fig. 8b. The corrosion process is almost active in nature but

8

there is a somewhat passive region extending from the rest potential of 0.117 V to the breakdown potential of 0.240 V resulting in a value of $E_B - E_R = 0.123$ V. This small value for $E_B - E_R$ is in contrast to the value of $E_B - E_R = 0.560$ V obtained from type "a" behaviour indicated above and indicates a sensitivity towards pitting corrosion and an increased corrosion rate. Further, the large hysteresis in the cyclic polarization curve for type "b" suggests little resistance towards crevice corrosion.

A typical cyclic polarization curve for alloy C22 in 10 wt% $FeCl_3$ at pH = 0.0 is given in Fig. 9. This polarization curve demonstrates that alloy C22 has excellent resistance to both pitting and crevice corrosion in this solution. It is worth noting that the parameters for corrosion of alloy C22 in 10 wt% $FeCl_3$ at pH = 0.0 are very similar to those for corrosion of alloy C22 in the much less aggressive 3.5 wt% NaCl solution at pH = 7.0 (Table 2 and Table 4).

One of the cyclic polarization curves for alloy C22 in 10 wt% $FeCl_3$ solution at pH = 0.0 exhibited a tendency towards active-passive behaviour as shown in Fig. 10 but the trend was small with the current at the Flade potential ($\approx$ -0.200 V vs SCE) being only about $1/10^{th}$ that of the passive current density. However, this trend towards active corrosion is consistent with the calculations of Lillard et al [6] who suggest that a pH in the range -0.25 to -0.50 could depassivate alloy 625 which has a composition similar to that of alloy C22.

It is interesting to note that the presence of 8.57 at% Mo in alloy C22 has the effect of both increasing the pitting potential and essentially eliminating hystereses in the cyclic polarization curves over those for the Mo free alloy 601 (Table 2 and Table 4). Additions of 2.0 at% Mo or higher to Co-24 at% Cr alloys eliminate the hysteresis from cyclic polarization curves when tested in 0.17 M NaCl solution (pH = 7.4) at 37 ^{o}C [11]. However, additions of Mo had no effect on the pitting potentials of the Co-Cr alloys. Also, additions of up to 5 at% Mo to

austenitic stainless steels tested in Ringers physiological solution at 37 °C increase the pitting potentials significantly over Mo-free alloys indicating an increased resistance to pitting corrosion. However, the additions of Mo did not reduce the large hysteresis in the cyclic polarization curves of these alloys and therefore the Mo-bearing austenitic stainless remain susceptible to crevice corrosion. Why additions of Mo to Ni-Cr and Co-Cr alloys essentially eliminate the hysteresis on the cyclic polarization curves thus increasing the resistance to crevice corrosion whereas additions of Mo to austenitic stainless steels do not eliminate or reduce the hysteresis remains puzzling.

Conclusions

For tests conducted in 3.5 wt% NaCl solution at pH = 7.0.

1. Alloy 600, alloy 601 and alloy C22 all exhibit passive behaviour with low corrosion rates (< 0.06 mmpy;

2. The increased Cr content in alloy 601 (25 at%) over alloy 600 (17 at%) increases the pitting potential thus increasing the resistance to pitting corrosion;

3. The presence of 8.57 at% Mo in alloy C22 increases the pitting potential of alloy C22 over that of alloy 601 thus indicating increased resistance to pitting corrosion;

4. Both alloys 600 and 601 exhibit large hysteresis in the cyclic polarization curves indicating a susceptibility to crevice corrosion;

5. Alloy C22 exhibits little hysteresis in the cyclic polarization curves indicating good resistance to crevice corrosion.

For tests conducted in HCl at pH =0.0

1. Both alloys 600 and 601 exhibited active corrosion polarization curves with resultant high corrosion rates;

2. Alloy C22 exhibited passive behaviour with low corrosion current densities, high pitting potentials, and very limited hysteresis on the cyclic polarization curves. In containment of HCl at pH = 0.0, this alloy would be expected to have a low corrosion rate and good resistance to both pitting and crevice corrosion.

For tests conducted in 10 wt% FeCl$_3$ solution at pH =0.0

1. Alloy 600 exhibited active corrosion behaviour with a high corrosion rate of over 3 mmpy.

2. Alloy 601 exhibited two types of polarization behaviour. One type of behaviour was similar to that for alloy 601 tested in 3.5 wt% NaCl at pH = 7.0. Corrosion current densities were low and pitting potentials were high indicating low corrosion rates and good resistance to pitting corrosion. However, the large amount of hysteresis for the cyclic polarization curves would indicate a susceptibility to crevice corrosion.

3. The second type of polarization behaviour for alloy 601 in 10 wt% FeCl$_3$ solution at pH =0.0 was almost active in nature with a passive region extending only about 200 mv above the corrosion potential and large hysteresis on the cyclic polarization curve. This polarization behaviour would suggest a susceptibility to both pitting and crevice corrosion.

4. Alloy C22 exhibited passive polarization behaviour with a high pitting potential and minimal hysteresis on the cyclic polarization curve. This alloy should be suitable for containment of 10 wt% FeCl$_3$ solution at pH = 0.0 with a minimum of pitting and crevice corrosion.

5. A slight tendency for active passive behaviour of alloy C22 in the FeCl3 solution indicates that perhaps at pH values lower than 0.0, some corrosion could occur.

Acknowledgment

References

[1] "Effect of Fluoride Ions on Crevice Corrosion and Passive Behavior of Alloy 22 in Hot Chloride Solutions", R.M. Carranza, M.A. Rodriguez, and R. B. Rebak*; Corrosion,* **63,** 5, pp. 480-490, 2007.

[2] "Crevice Corrosion Penetration Rates of Alloy 22 in Chl;oride-Containing Waters"X. He and D.S. Dunn;, *Corrosion*, **63**, 2, pp.145-158, 2007.

[3] "Crevice Corrosion Stabilization and Repassivation Behavior of Alloy 625 and Alloy 622", B.A. Kehler, G.O. Ilevbare, and J.R. Scully; *Corrosion*, **57**, 12, pp.1042-1065, 2001.

[4] "Cr, Mo and W alloying additions in Ni and their effect on passivity", Amy C. Lloyd, James J. Noël, Stewart McIntyre, David Shoesmith;, *Electrochimica Acta*, **49**, pp. 3015-3027, 2004.

[5] "Assessment of Corrosion Resistance and Metal Ion Leaching of Nitinol Alloys", Waseem Haider and Norman Monroe; *Journal of Materials Engineering and Performance*, **20,** 4-5, pp. 812-815, 2011.

[6] "Crevice Corrosion of Alloy 625 in Chlorinated ASTM Artificial Ocean Water", R.S. Lillard, M.P. Jurinski, and J. R. Scully;, *Corrosion,* **50**, 4, pp. 251-265, 1994.

[7] "Acoustic Emission During Corrosion", J,R. Cahoon, M.N. Bassim, and E. Gennelle Oman, *Canadian Metallurgical Quarterly*, **25,** 1, pp. 73-77, 1986.

[8] "Non-Ferrous Alloys and Special Purpose Materials", *ASM Handbook*, 2; Properties and Selection: ASM International, **2**, pp. 438-439. 1990.

[9] "Electron Configuration and Ionization Energy of Neutral Atoms in the Ground State", in CRC Handbook of Chemistry and Physics, 92nd Edition (Internet Version 2012), W. M. Haynes. ed., CRC Press/Taylor and Francis, Boca Raton, FL.

[10] "The Engel-Brewer Theories of Metals and Alloys," W. Hume-Rothery; *Progr. Mater. Sci.*, **13**, pp. 229-265, 1967.

[11] "The Susceptibility of Metallic Surgical Implant materials to Crevice Corrosion", J. R. Cahoon and C. T. F. Cheung;, *Canadian Metallurgical Quarterly*, **21,** 3, pp. 289-292, 1982.

[12] "Effect of Composition on the Electrochemical Behaviour of Austenitic Stainless Steels In Ringer's Solution", R. Bandy and J. R. Cahoon; *Corrosion*, **33**, 6, pp. 204-208, 1977.
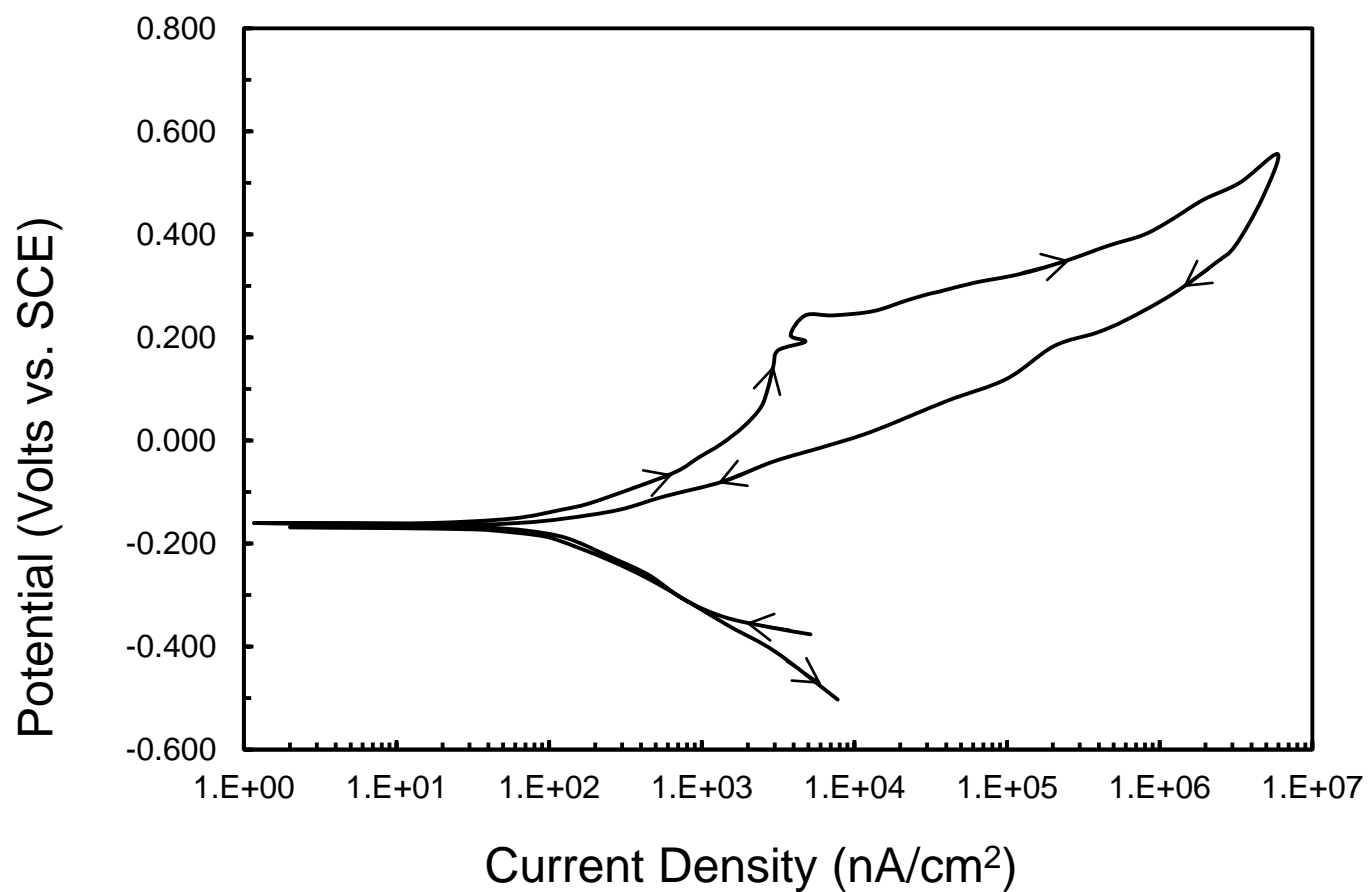
List of Figures

Fig. 1 Cyclic anodic polarization curve for alloy 600 in 3.5%NaCl solution at pH = 7.0.
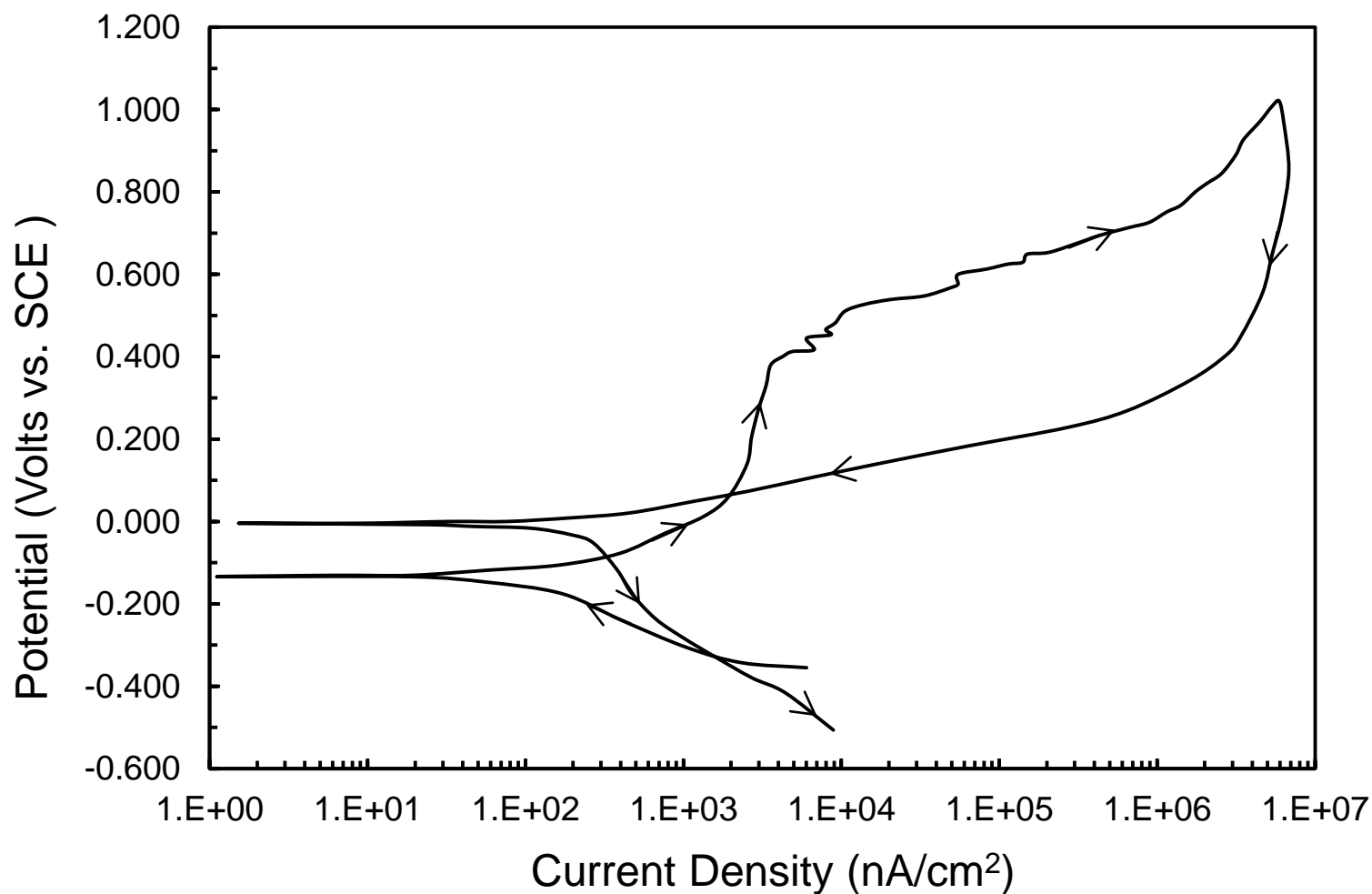
15

Fig 2. Cyclic anodic polarization curve for alloy 601 in 3.5%NaCl solution at pH = 7.0.
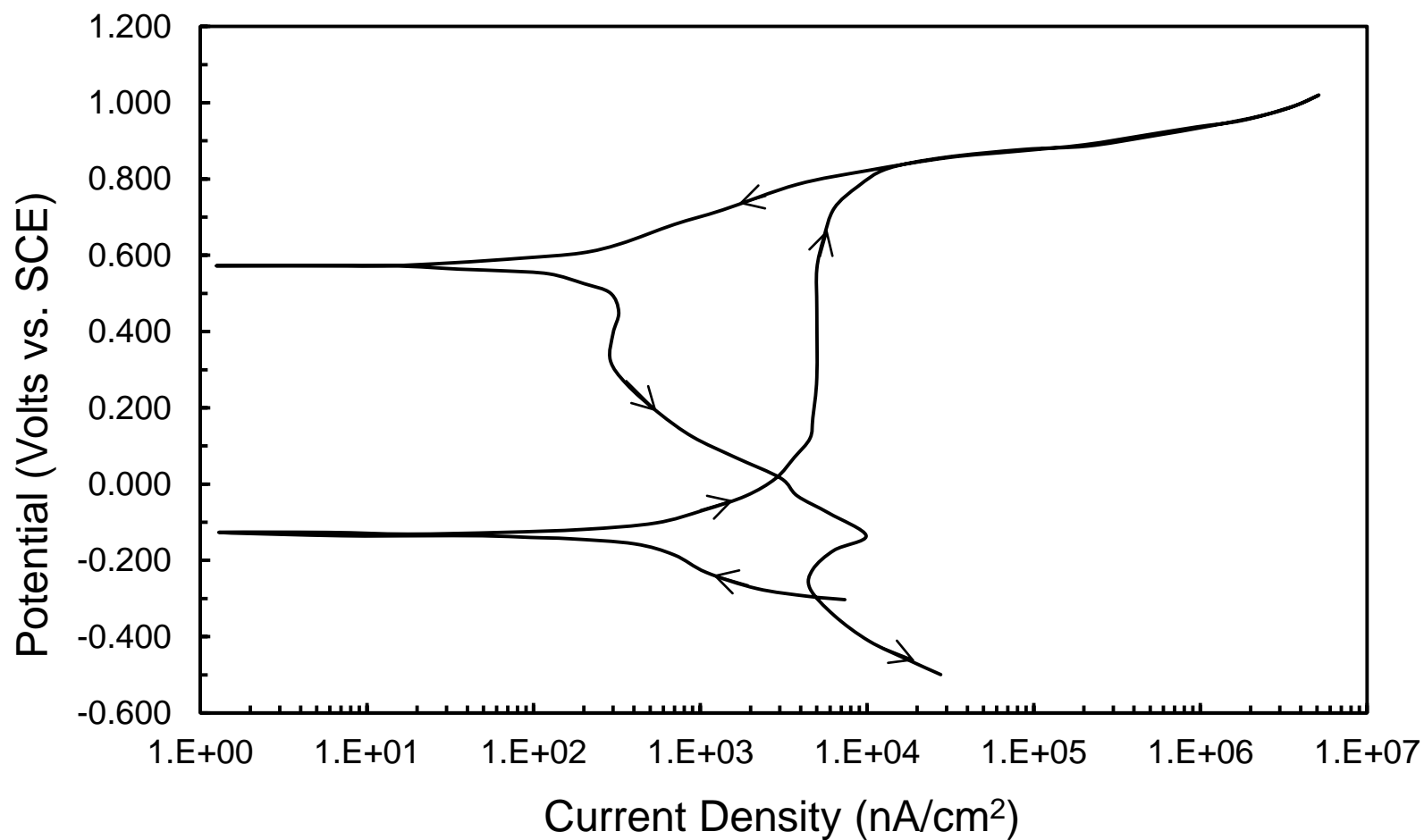
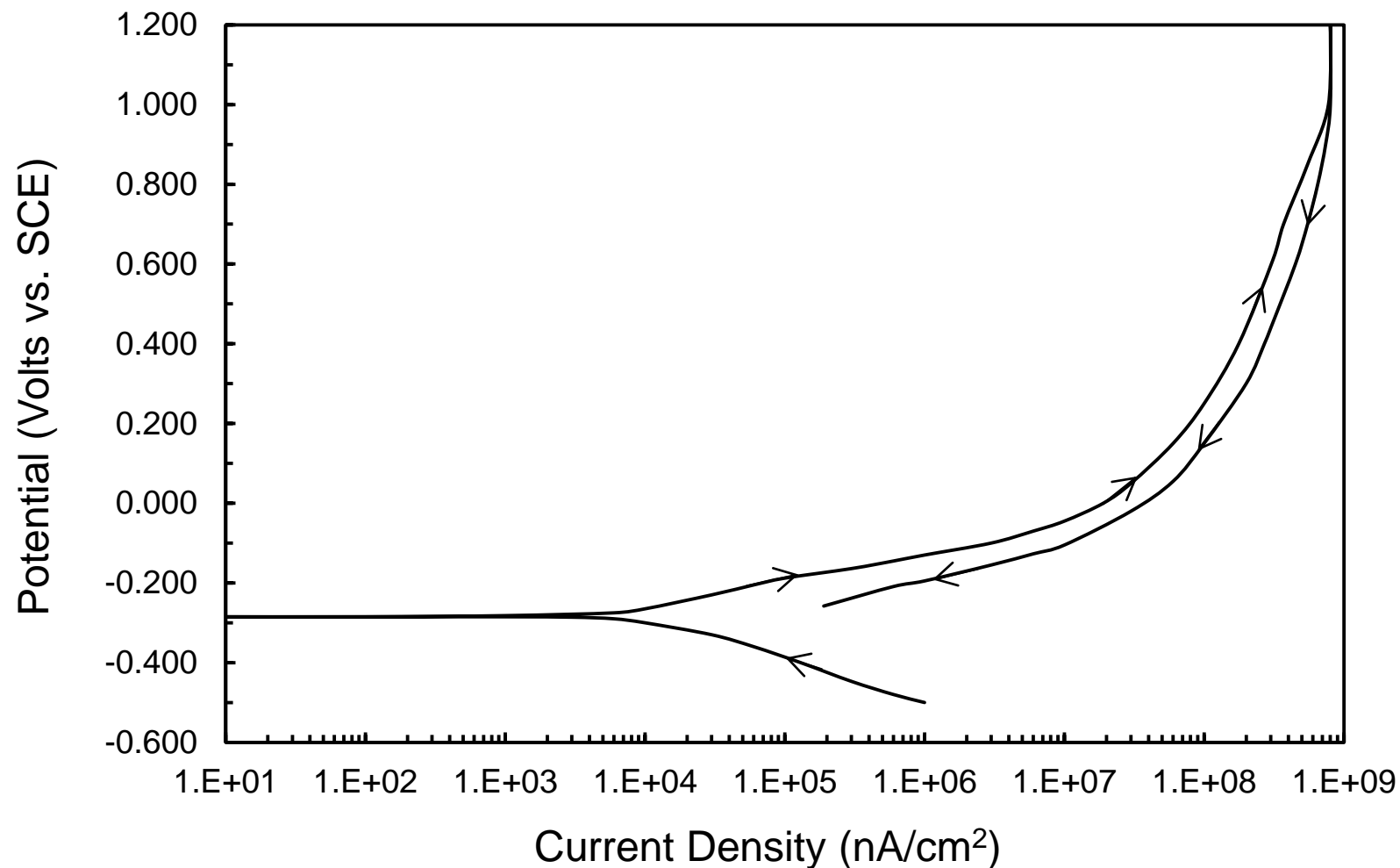Fig. 3. Cyclic anodic polarization curve for alloy C22 in 3.5% NaCl solution at pH = 7.0.

Fig. 4. Cyclic anodic polarization curve for alloy 600 in HCl at pH = 0.0.
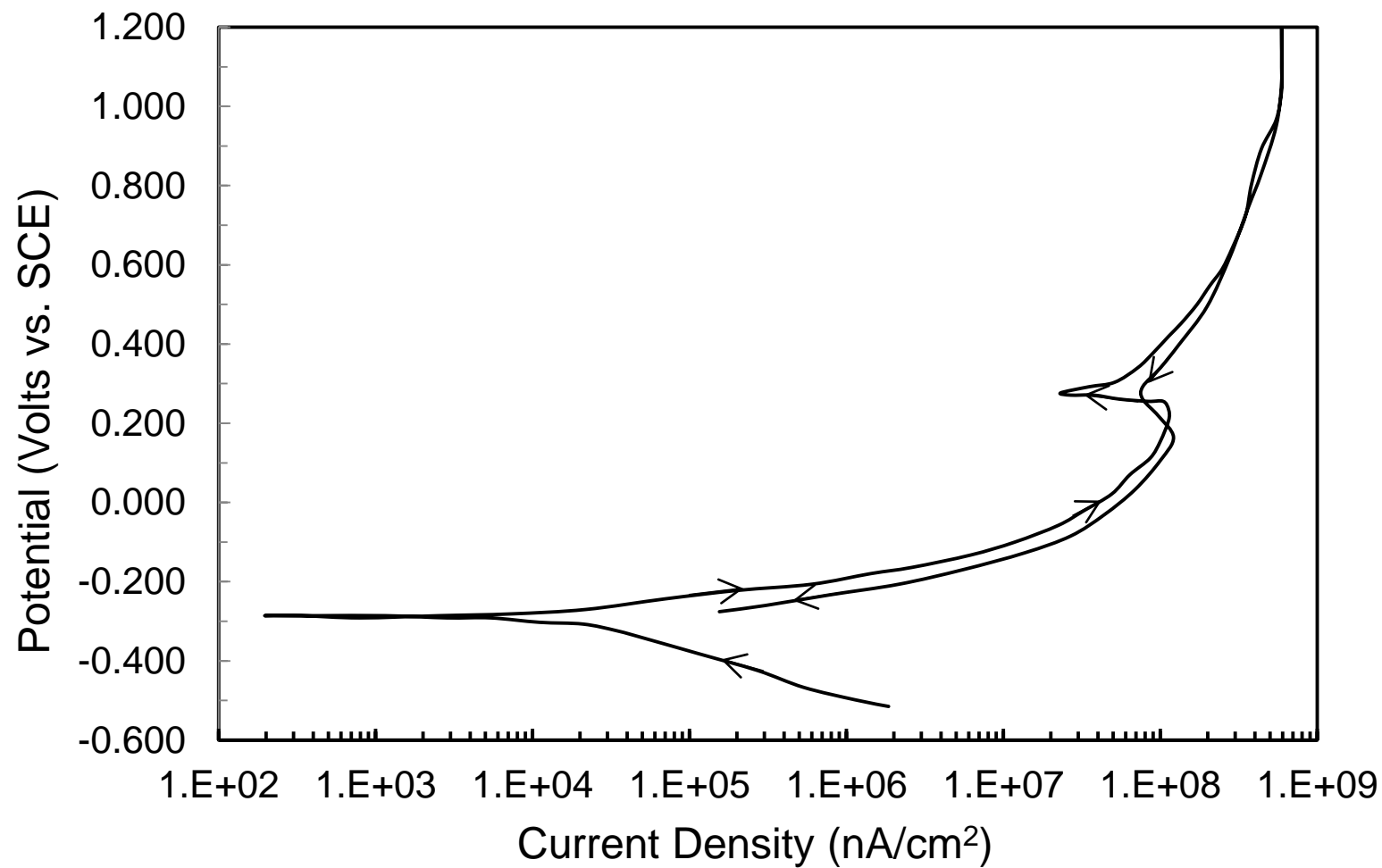
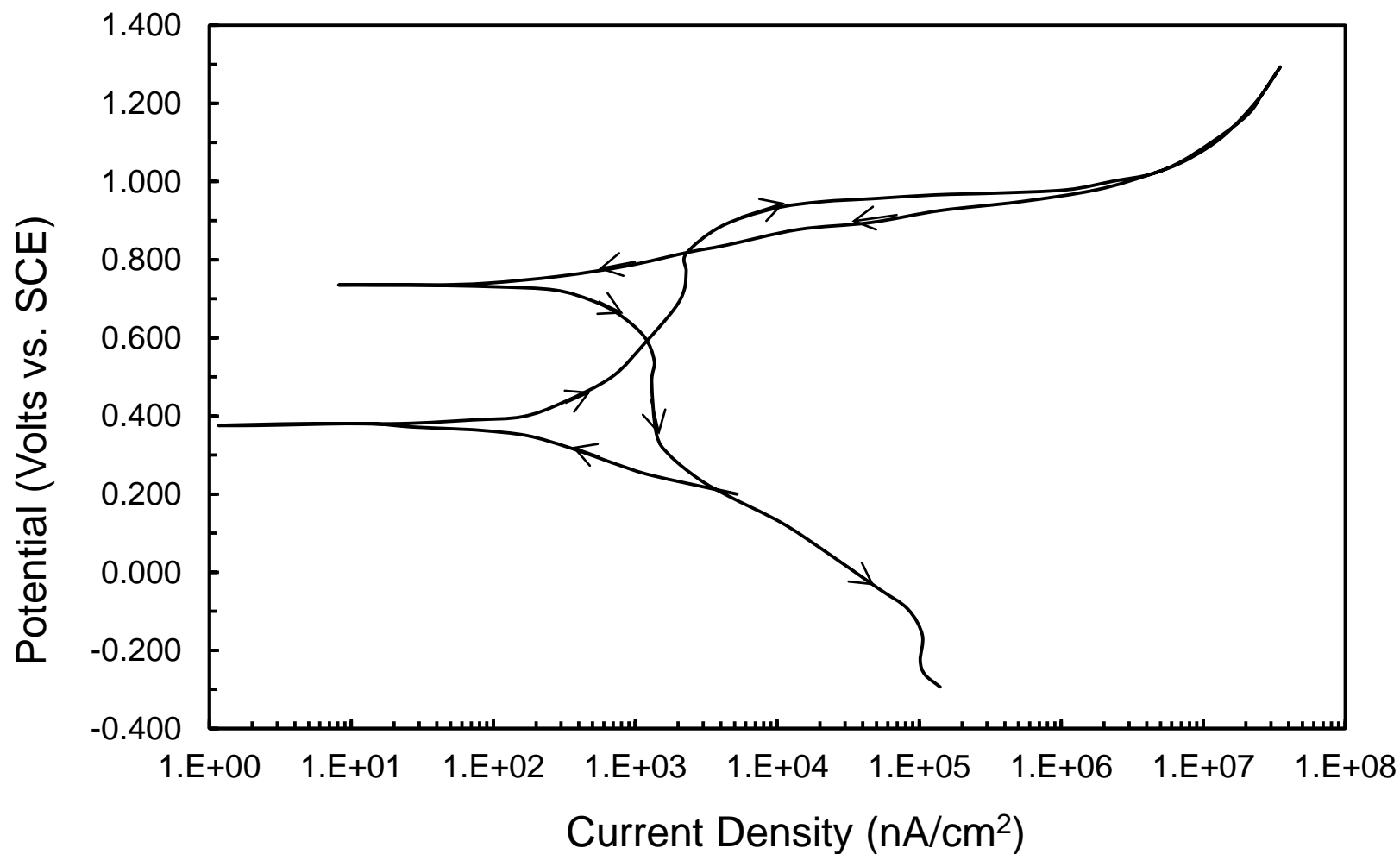Fig. 5. Cyclic anodic polarization curve for alloy 601 in HCl at pH = 0.0.

Fig. 6. Cyclic anodic polarization curve for alloy C22 in HCl at pH = 0.0.
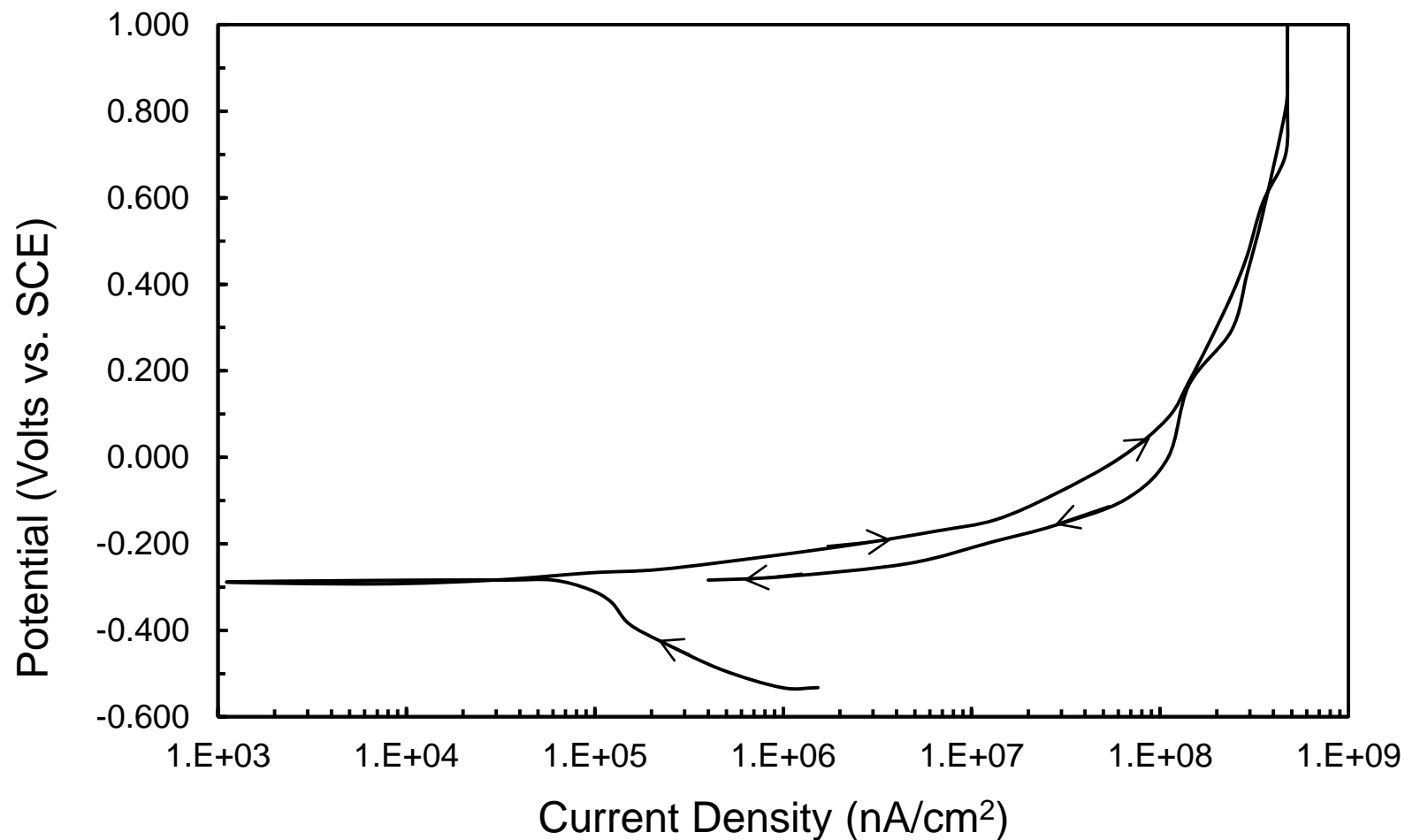
Fig. 7. Cyclic anodic polarization curve for alloy 600 in 10 wt. % FeCl$_3$ at pH = 0.0.

Fig. 8 a. The first of two types of cyclic anodic polarization curves for alloy 601 in 10 % FeCl$_3$

solution at pH = 0.0.

22
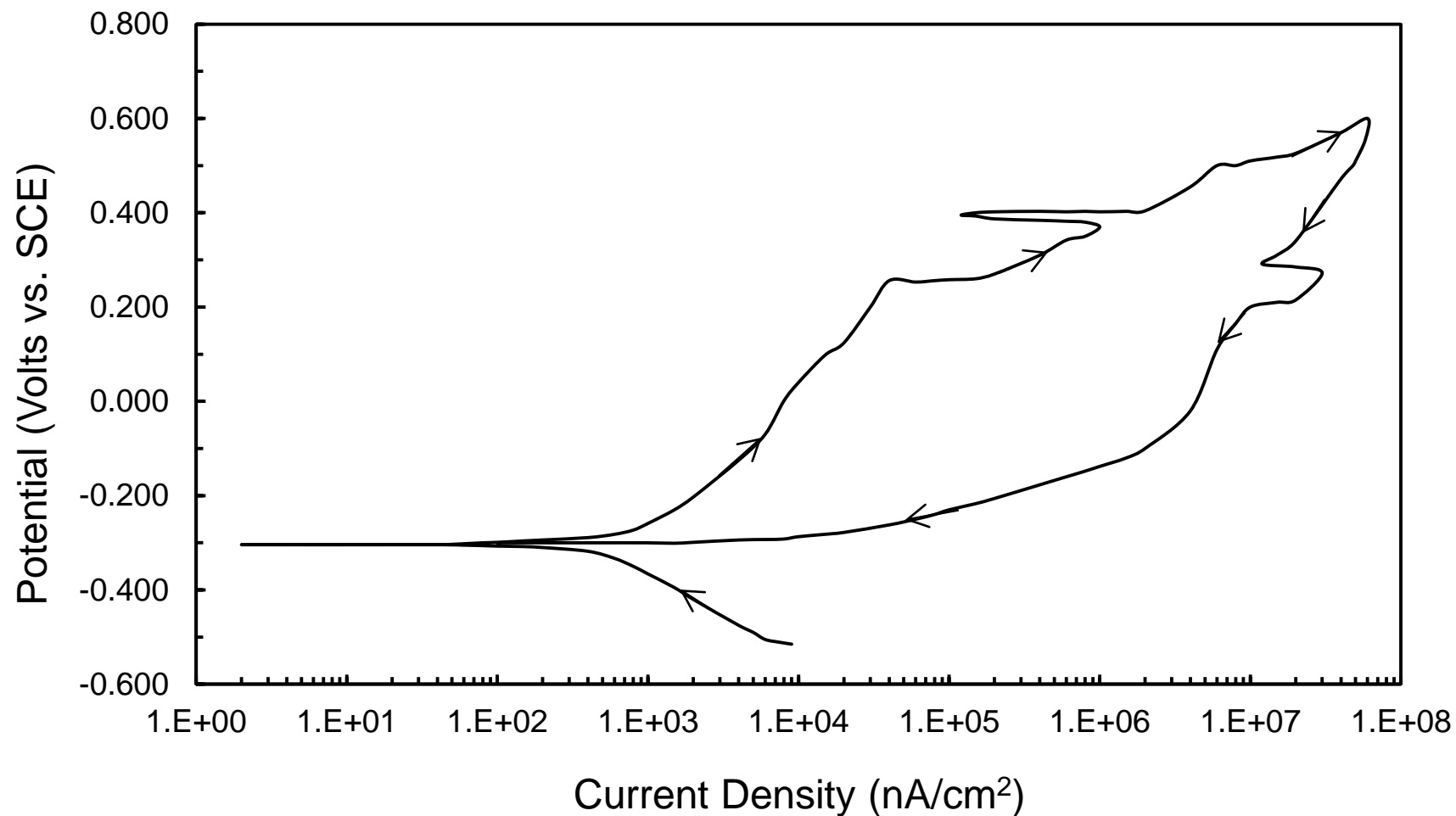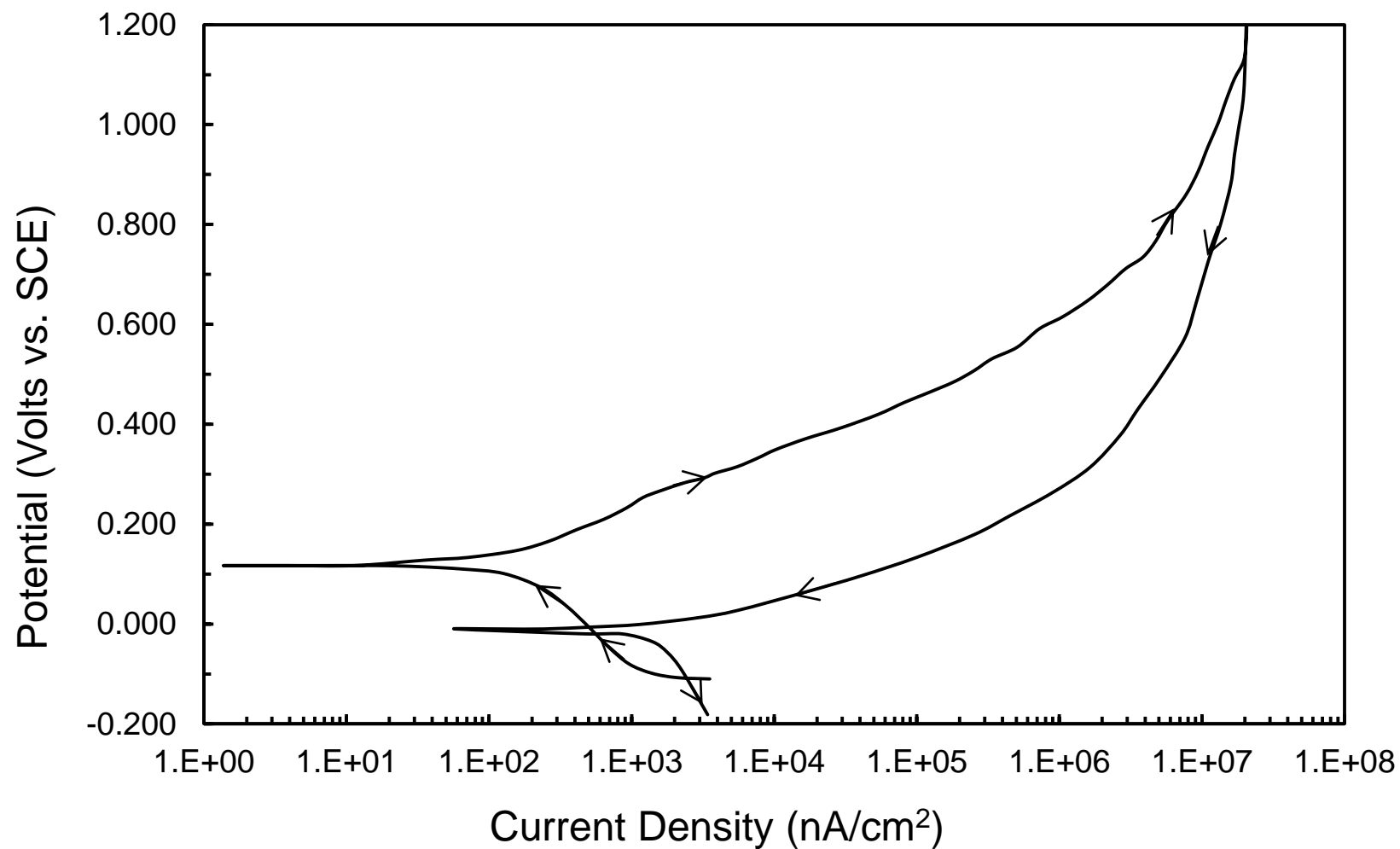
Fig. 8 b. The second of two types of cyclic anodic polarization curves for alloy 601 in 10 % FeCl$_3$
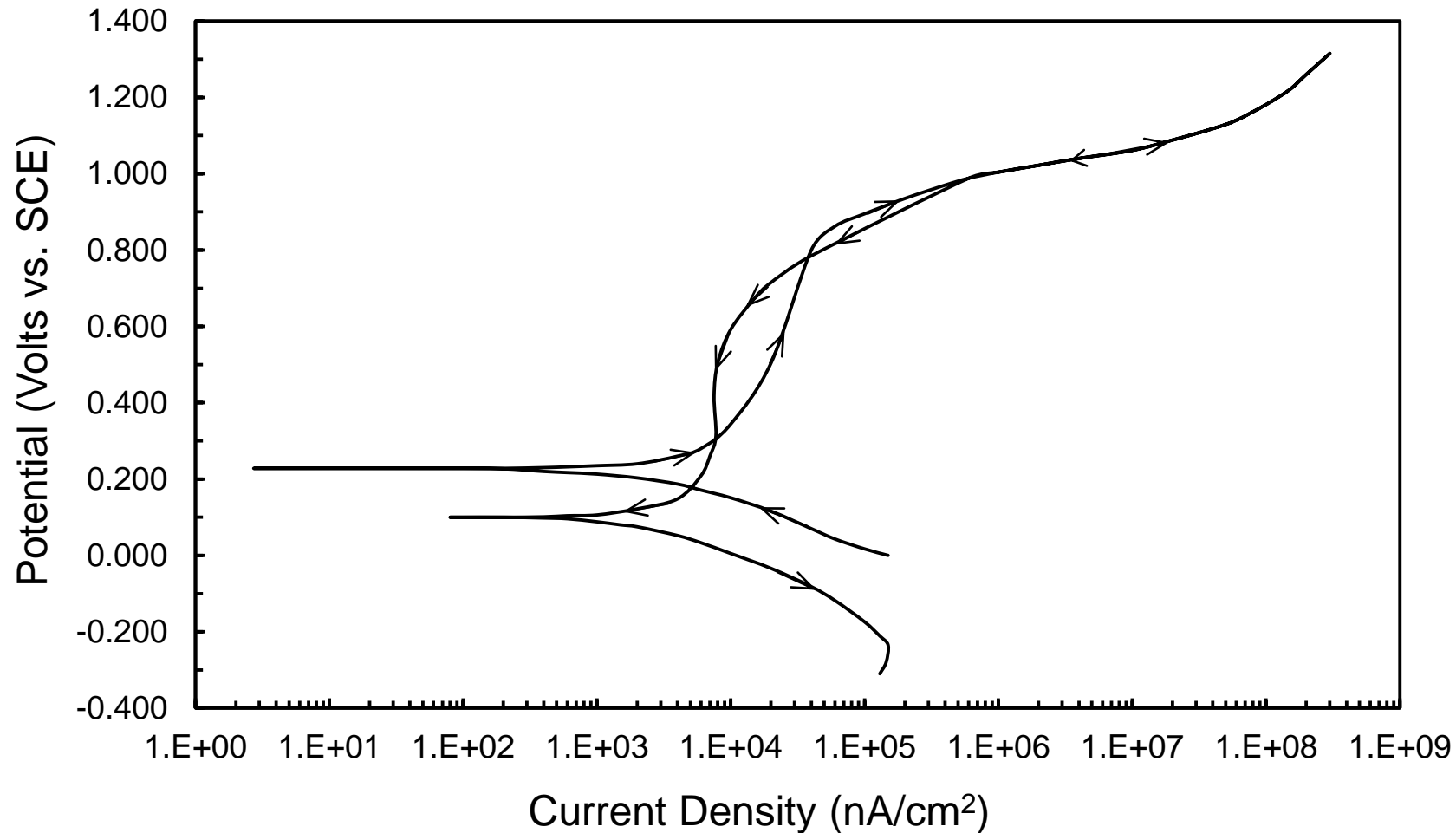
solution at pH = 0.0

Fig. 9. Cyclic anodic polarization curve for alloy C22 in 10 % FeCl$_3$ solution at pH= 0.0.
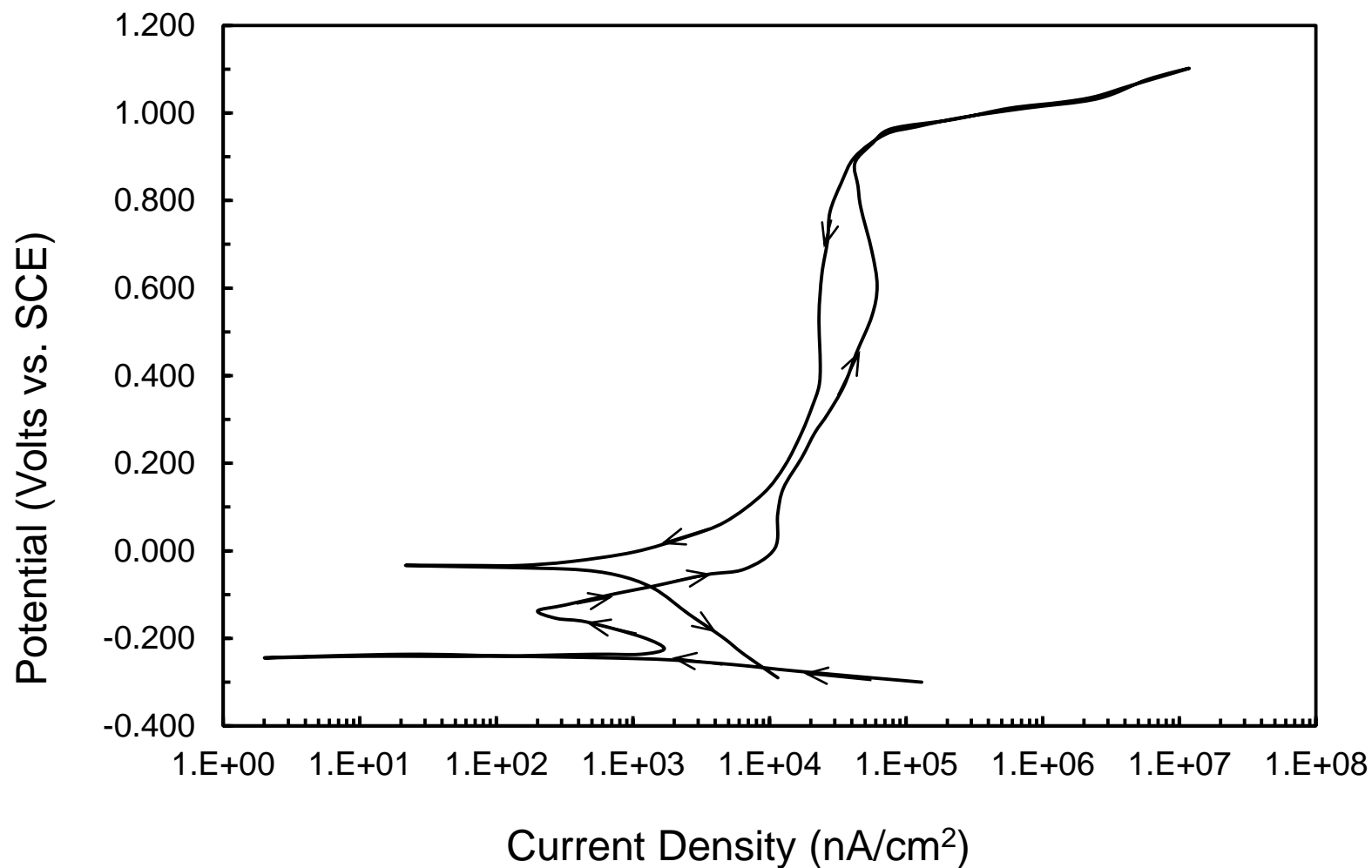
Fig. 10. Cyclic anodic polarization curve for alloy C22 in 10 % FeCl₃ solution at pH = 0.0

showing a tendency towards active-passive behavior.

List of Tables

Table 1. Nominal compositions of the alloys and values used for calculation of physical properties.

Table 2. Summary of anodic polarization parameters for alloys tested in 3.5 wt. % NaCl solution at pH = 7.0, HCl acid at pH = 0.0, and 10 wt. % $FeCl_3$ solution at pH = 0.0.

Table 3. Values used to calculate corrosion rate.

Table 4. Summary of resistance to pitting and crevice corrosion for alloys tested in 3.5 wt. % NaCl solution at pH = 7.0, HCl acid at pH = 0.0, and 10 wt. % $FeCl_3$ solution at pH = 0.0.

Table 1. Nominal compositions of the alloys and values used for calculation of physical properties.

		Ni	Cr	Fe	Mo	W	Co	Al	Mn	Si	V	C
						Element						
At. Wt. (g/mole)		58.69	52.00	55.85	95.94	183.85	58.93	29.98	54.94	28.09	50.94	12.01
Density (g/cm^3)		8.91	7.14	7.87	10.25	19.25	8.90	2.70	7.47	2.33	6.11	2.27
Oxidation State		2.00	2.00	2.00	2.00	2.00	2.00	3.00	2.00	4.00	2.00	4.00
Alloy												
600	Wt%	75.72	15.50	8.00	###	###	###	###	0.50	0.20	###	0.08
	At%	73.54	16.99	8.16	###	###	###	###	0.52	0.41	###	0.38
601	Wt%	60.72	23.00	14.10	###	###	###	1.40	0.50	0.20	###	0.08
	At%	57.51	24.59	14.03	###	###	###	2.60	0.51	0.40	###	0.37
C22	Wt%	50.69	21.50	5.50	13.50	4.00	2.50	###	1.00	1.00	0.30	0.01
	At%	52.63	25.19	6.00	8.57	1.33	2.59	###	1.11	2.17	0.36	0.05

Table 2. Summary of anodic polarization parameters for alloys tested in 3.5 wt% NaCl solution at pH = 7.0, HCl acid at pH 0.0, and 10 wt % $FeCl_3$ solution at pH 0.0.

Solution	Alloy	^1E_R (V vs SCE)	^2E_B (V vs SCE)	$^3I_{CORR}$ (nA/cm^2)	Corrosion Rate (mm/year)	$^4I_{PASS}$ (nA/cm^2)	Polariz. Behav.	Amount of Hysteresis	^5E_P (V vs SCE)
3.5 wt %	600	-0.159	0.239	1.31×10^2	0.029	1.92×10^3	Passive	Large	0.014
NaCl	601	-0.107	0.383	0.93×10^2	0.023	2.10×10^3	Passive	Large	0.007
pH = 7.0	C22	-0.109	0.627	1.78×10^2	0.051	4.40×10^3	Passive	None	0.656
HCl	600	-0.304	NA	1.20×10^4	0.131	NA	Active	NA	NA
Acid	601	-0.197	NA	2.39×10^4	0.263	NA	Active	NA	NA
pH=0.0	C22	0.143	0.951	0.57×10^2	0.009	0.76×10^3	Passive	Small	0.834
10 wt %	600	-0.234	NA	2.80×10^5	3.30	NA	Active	NA	NA
$FeCl_3$	601 a	-0.328	0.218	1.161×10^3	0.013	9.85×10^3	Passive	Large	-0.223
Solution	601 b	-0.035	0.182	1.047×10^4	0.230	1.73×10^4	Passive	Large	0.029
pH = 0.0	C22	0.031	0.794	2.74×10^3	0.032	2.77×10^4	Passive	Small	0.741

^1E_R, Rest or corrosion potential; ^2E_B, Breakdown or pitting potential; $^3I_{CORR}$, Corrosion current density; $^4I_{PASS}$, Passive current density; ^5E_P, Protection potential.

Table 3. Values used to calculate corrosion rate.

Alloy	At. Wt. g/mole	Density (g/cm^3)	Oxidation State
600	57.00	8.46	2.02
601	55.59	8.11	2.04
C22	60.94	8.48	2.04

Table 4. Summary of resistance to pitting and crevice corrosion for alloys tested in 3.5 wt% NaCl solution at pH = 7.0, HCl acid at pH 0.0, and 10 wt % $FeCl_3$ solution at pH 0.0.

Solution	Alloy	$E_B - E_R$	$E_P - E_R$
3.5 wt %	600	0.398	0.173
NaCl	601	0.490	0.114
pH = 7.0	C22	0.736	0.765
HCl	600	NA	NA
Acid	601	NA	NA
pH=0.0	C22	0.808	0.691
10 wt %	600	NA	NA
$FeCl_3$	601 a	0.512	0.046
Solution	601 b	0.181	0.128
pH = 0.0	C22	0.763	0.710